CSIRO PUBLISHING

Sixth Torino Workshop

www.publish.csiro.au/journals/pasa *Publications of the Astronomical Society of Australia*, 2003, **20**, 389–392

Low-Mass AGB Stellar Models for $0.003 \leq Z \leq 0.02$: Basic Formulae for Nucleosynthesis Calculations

O. Straniero[1], I. Domínguez[2], S. Cristallo[3] and R. Gallino[4,5]

[1] INAF, Osservatorio Astronomico di Teramo, Italy
straniero@te.astro.it
[2] Universidad de Granada, Spain
inma@ugr.es
[3] INAF, Osservatorio Astronomico di Teramo, Italy
cristallo@te.astro.it
[4] Dip. Fisica Generale Università di Torino and Sez. INFN Torino, Italy
gallino@ph.unito.it
[5] Center for Stellar and Planetary Astrophysics, Monash University, Melbourne 3800, Australia

Received 2003 June 17, accepted 2003 October 24

Abstract: We have extended our published set of low-mass AGB stellar models to lower metallicities. Different mass-loss rates have been explored. We provide interpolation formulae for the luminosity, effective temperature, core mass, mass of dredge up material and maximum temperature in the convective zone generated by thermal pulses. Finally, we discuss the resultant modification of these quantities when we use an appropriate treatment of the inward propagation of the convective instability, as caused by the steep rise in radiative opacity when the convective envelope penetrates the H-depleted region.

Keywords: stars: abundances — stars: AGB — stars: evolution — nucleosynthesis

1 Introduction

Results from detailed Asymptotic Giant Branch (AGB) stellar models demonstrate that low-mass AGB stars (i.e. $1.3 \leq M/M_{\odot} \leq 3$) produce the majority of cosmic s-process elements (Straniero et al. 1995; Gallino et al. 1998; Busso et al. 1999). Such a scenario has been confirmed by measurements of the chemical composition of AGB stars (Lambert et al. 1995; Busso et al. 2001; Abia et al. 2001, 2002) and by analysis of the isotopic composition of meteoritic SiC grains (Gallino et al. 1997).

The present generation of AGB stars, as observed in the disk of our Galaxy, has a nearly solar chemical composition. However, the SiC grains found in pristine meteorites originated in the carbon-rich circumstellar envelopes of a pre-solar generation of AGB stars, whose original metallicity could have been somewhat lower than that of solar-system material. In addition, an important contribution to our understanding of AGB stars comes from observations of the stellar populations in the fields of the Small and Large Magellanic Clouds, whose respective mean metallicities are about one-fifth and one-half solar. In a previous paper (Straniero et al. 1997) the properties of low-mass AGB stellar models, with solar composition, are extensively discussed. Here we present an extension of these models to lower metallicities.

2 The Grid of Models and Interpolations

The full grid of models is summarised in Table 1. The corresponding AGB evolutionary sequences have been obtained from the FRANEC code, as described in Straniero et al. (1997). The initial mass (M, in units of $M_{\odot}$), helium content (Y) and metallicity (Z, i.e. the initial mass fraction of elements with $A \geq 12$) are listed in Table 1. Various mass-loss rates ($\dot{M}$) have been applied during the AGB phase. In all cases we have used the Reimers formula (Reimers 1975):

Table 1. The Computed Grid of Models

$M\ (M_{\odot})$	Y	Z	η	β
1.0	0.280	0.020	0	0
1.5	0.280	0.020	0	0
1.5	0.280	0.020	0.4	0/0.1
2.0	0.280	0.020	0.4	0/0.1
3.0	0.280	0.020	0	0
3.0	0.280	0.020	1.5	0/0.1
1.5	0.255	0.006	0.5	0/0.1
3.0	0.255	0.006	1.5	0
1.5	0.230	0.003	0.4	0/0.1
3.0	0.230	0.003	1.5	0

$$\dot{M}\ (M_{\odot}\ \mathrm{yr}^{-1}) = 1.34 \times 10^{-5} \eta \frac{L^{3/2}}{M T_{\mathrm{eff}}^2} \qquad (1)$$

where η is a free parameter, L is in units of $L_{\odot}$, and T_{eff} is the effective temperature. We have not considered mass loss in pre-AGB evolution, because in the mass range 1.5–3.0 $M_{\odot}$, just a few hundredths of $M_{\odot}$ are expected to be lost. For example, by adopting $\eta = 0.4$ as representative of the pre-AGB mass-loss rate (e.g. Fusi Pecci & Renzini 1976), we find that the total mass lost before the onset of the AGB phase by a 2 $M_{\odot}$ star, with solar composition, should be 0.04 $M_{\odot}$. Clearly, such a small amount of

© Astronomical Society of Australia 2003

10.1071/AS03041 1323-3580/03/04389

Downloaded from https://www.cambridge.org/core. IP address: 54.174.225.82, on 22 Jan 2022 at 10:02:55, subject to the Cambridge Core terms of use, available at https://www.cambridge.org/core/terms. https://doi.org/10.1071/AS03041

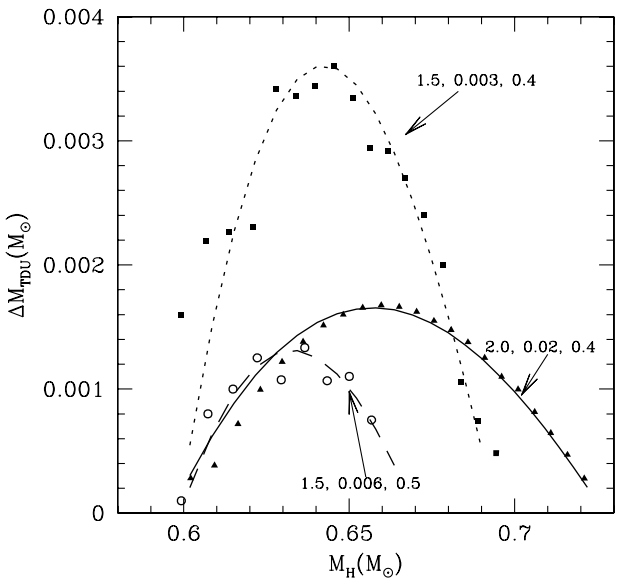

Figure 1 $\Delta M_{\rm TDU}$ per thermal pulse, as a function of $M_{\rm H}$, for three evolutionary sequences. Triangles indicate a $M = 2.0\ M_\odot$, $Z = 0.02$ and $\eta = 0.4$ FRANEC model, with the interpolation formula as a solid line. Circles indicate a $M = 1.5\ M_\odot$, $Z = 0.006$ and $\eta = 0.5$ FRANEC model, with the interpolation formula as a dashed line. Squares indicate a $M = 1.5\ M_\odot$, $Z = 0.003$ and $\eta = 0.4$ FRANEC model, with the interpolation formula as a dotted line.

mass loss has negligible consequences on the pre-AGB evolution.

The thermally pulsing AGB (TP-AGB) models are characterised by three distinct phases:

- The *early phase* includes the first few (gentle) thermal pulses (TPs), which are not followed by the third dredge-up (TDU);
- The *TDU phase* begins when the mass of the H-exhausted core becomes as large as 0.59–0.6 $M_\odot$. The amount of mass dredged up ($\Delta M_{\rm TDU}$) first increases, as the core mass ($M_{\rm H}$) increases, and then decreases, when the envelope mass ($M_{\rm env}$) is substantially reduced;
- During the *final phase* of the AGB the concurrent action of mass loss and H burning erodes the envelope and the TDU ceases. The minimum $M_{\rm env}$ for the occurrence of the TDU is about 0.4–0.5 $M_\odot$.

Figure 1 shows the variation of $\Delta M_{\rm TDU}$, as a function of $M_{\rm H}$, for some selected models.

An interpolation on the grid of models provides useful analytic expressions for relevant quantities, as a function of $M_{\rm H}$, $M_{\rm env}$ and Z. In the following we report the result of these interpolations.

- The time elapsed between two successive TPs (the interpulse period) is

$$\Delta t_{\rm ip}(10^5\ {\rm yr}) = 18.5178 - 59.8876 M_{\rm H} + 48.8462 M_{\rm H}^2 - 4.0273 \log Z + 5.8422 M_{\rm H} \log Z \quad (2)$$

This is valid for $M_{\rm H} \geq 0.58$. For smaller $M_{\rm H}$, substitute $M_{\rm H}$ by $(1.16 - M_{\rm H})$. The standard deviation of this fit (σ, i.e. the average difference between the values calculated with the fitting formula and those of the models) is 0.01.

- The mass of H-depleted material dredged up in a given TDU episode is

$$\begin{aligned}\Delta M_{\rm TDU}/M_\odot = {} & [1.0 + 0.21 \log(Z/Z_\odot) \\ & + 6.3 \log^2(Z/Z_\odot)] \\ & \times \left[-6.210^{-4} + 9.110^{-4} M_{\rm env}\right. \\ & - 3.710^{-4} M_{\rm env}^2 \\ & + 5.06110^{-2} M_{\rm env} \delta M_{\rm H} \\ & - 5.9610^{-3} M_{\rm env}^2 \delta M_{\rm H} \\ & - 3.837210^{-1} M_{\rm env} \delta M_{\rm H}^2 \\ & \left. + 9.44810^{-2} M_{\rm env}^2 \delta M_{\rm H}^2\right] \end{aligned} \quad (3)$$

where $Z_\odot = 0.02$, $\delta M_{\rm H} = M_{\rm H} - M_{\rm H}^*$ and $M_{\rm H}^*$ is $M_{\rm H}$ at the last TP without TDU (the last pulse of the *early phase*). For the masses and chemical compositions we have considered, $M_{\rm H}^*$ lies between 0.59 and 0.60. The curves plotted in Fig. 1 have been obtained by using $M_{\rm H}^* = 0.595$. When $M_{\rm env} < 0.4$ or $\delta M_{\rm H} \leq 0$, $\Delta M_{\rm TDU}$ is effectively 0. For this fitting formula, $\sigma = 2 \times 10^{-4}$.

- The luminosity at half of $\Delta t_{\rm ip}$ is

$$\log \frac{L}{L_\odot} = 3.603 + 6.7806 \Delta M_{\rm H} - 27.582 \Delta M_{\rm H}^2 + 277.333 \Delta M_{\rm H}^4 \quad (4)$$

$\Delta M_{\rm H} = M_{\rm H} - M_{\rm H}(t_0)$ and $M_{\rm H}(t_0)$ is $M_{\rm H}$ at the epoch of the first TP (t_0). The latter quantity depends on the metallicity: $M_{\rm H}(t_0) = 0.517 - 1.93910^{-2} \log Z$. For this fit $\sigma = 10^{-4}$.

- The effective temperature at half of $\Delta t_{\rm ip}$ is

$$\log T_{\rm eff} = 5.0475 + 0.1438 \log Z_{\rm eff} + 0.0513 \log^2 Z_{\rm eff} - 4.1895 M_{\rm H} + 2.9594 M_{\rm H}^2 \quad (5)$$

$Z_{\rm eff}$ is the effective metallicity, which includes the extra carbon in the envelope due to the TDU. The use of $Z_{\rm eff}$, instead of Z, has a minor effect on solar composition stars. However, it may significantly increase the estimated radius and, in turn, the mass loss rate, for stars with an initially low metal content. For this interpolation, $\sigma = 5 \times 10^{-4}$.

- The maximum temperature attained at the bottom of the convective zone generated by a TP is

$$\log T_{\rm max} = 6.7747 + 4.6856 M_{\rm H} - 3.21 M_{\rm H}^2 + 0.01 M_{\rm env} - 6.2337 Z + 7.87595 Z M_{\rm H} \quad (6)$$

For $\log T_{\rm max}$, $\sigma = 3 \times 10^{-3}$.

- Finally, the evolution of $M_{\rm H}$ during the whole TP-AGB phase may be estimated by means of the following formula:

$$M_{\rm H} = M_{\rm H}^* + 6.9 \cdot 10^{-3} k - 6.0 \times 10^{-5} k^2 \quad (7)$$

Downloaded from https://www.cambridge.org/core. IP address: 54.174.225.82, on 22 Jan 2022 at 10:02:55, subject to the Cambridge Core terms of use, available at https://www.cambridge.org/core/terms. https://doi.org/10.1071/AS03041

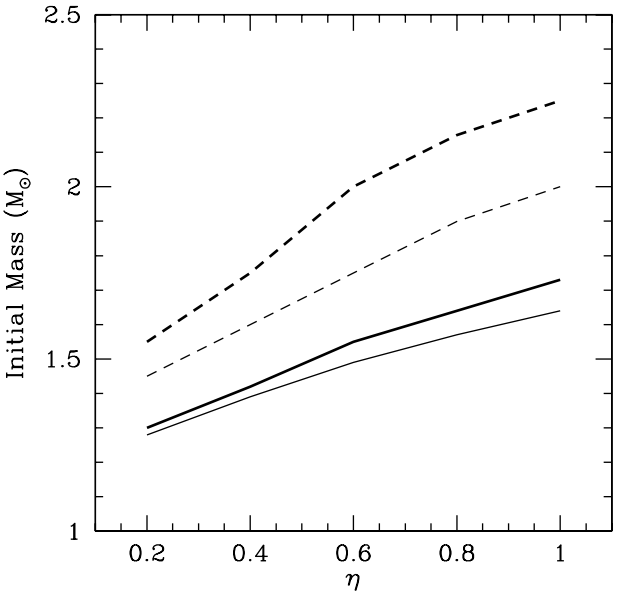

Figure 2 The minimum initial mass for the occurrence of the TDU (solid lines) and the minimum initial mass for C-star progenitors (dashed lines) as a function of $\dot{M}$ (η). η refers to the free parameter in the Reimers formula. These results are based on solar metallicity models ($Z = 0.02$ and $Y = 0.28$). Thick lines represent the case of models with minimal dredge up, while thin lines have been derived from models that include an exponential decline of the convective velocity at the boundaries of the convective zone (see Section 3).

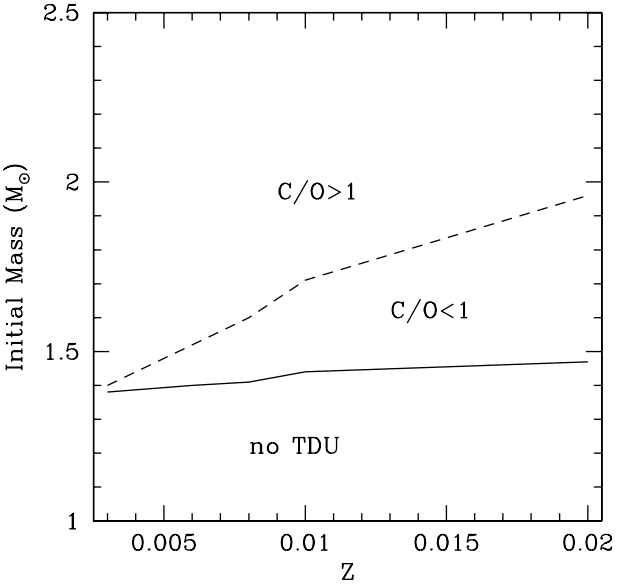

Figure 3 The minimum initial mass for the occurrence of the TDU (solid line) and the minimum initial mass for C-star progenitors (dashed line) as a function of Z. These results are based on models computed with a Reimers mass-loss rate ($\eta = 0.5$) and minimal dredge up (see Section 3).

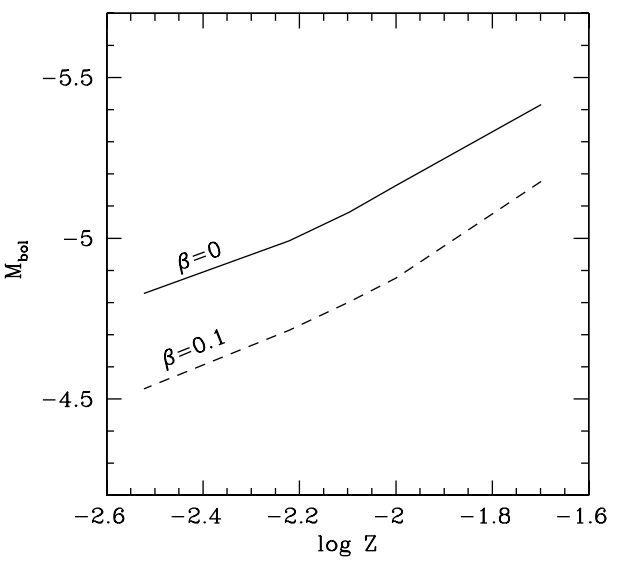

Figure 4 The minimum luminosity for a C-star as a function of Z. These results are based on models computed with a Reimers mass-loss rate ($\eta = 0.5$) and with (dashed line) and without (solid line) exponential decline of the convective velocity.

where $k = -n,\ -n+1,\ \ldots,\ 0,\ 1,\ \ldots,\ j$ and $k = 0$ corresponds to the last TP without TDU ($M_{\rm H} = M_{\rm H}^{*}$). The value of $n+1$ is the number of TPs during the *early phase*, while j is the number of TPs that occur from the first TDU episode up to the tip of the AGB (*TDU phase + final phase*). This formula gives $M_{\rm H}$ to within $5 \times 10^{-3}\, M_{\odot}$. Now, the envelope mass is easily obtained by $M_{\rm env} = M_{\rm tot} - M_{\rm H}$, where $M_{\rm tot}$ is the current stellar mass.

Note that, if the initial mass of the star is too small, the conditions for the activation of the TDU (namely, $M_{\rm H} \geq 0.60\, M_{\odot}$ and $M_{\rm env} \geq 0.4\, M_{\odot}$) are never reached. The minimum mass for the occurrence of the TDU, as a function of the mass loss rate, is shown in Fig. 2, for solar composition models. In stars with masses exceeding this lower limit, the envelope composition is modified by the TDU: ^{12}C and s-process elements are enhanced. Obviously, a carbon star may form, after a suitable number of TDU episodes, only if the initial mass is large enough. The dashed line in Fig. 2 shows, for solar metallicity models, the lower mass limit for the formation of a C-star as a function of η.

Both of these lower limits depend on the metallicity. The smaller the metallicity, the smaller the mass for the activation of the TDU phase and the lower the minimum initial mass for the formation of a C-star. This is illustrated in Fig. 3 (for $\eta = 0.5$).

At low metallicities (i.e. $Z < 4 \times 10^{-3}$), even taking into account an enhancement of the α-elements (as typically found in halo stars), the amount of oxygen in the envelope is so low that just one TDU episode is sufficient to increase the C/O ratio above unity. Correspondingly, $M_{\rm H}$ and the luminosity at C/O = 1 decrease at low Z (see Fig. 4).

3 The Efficiency of the TDU: Opacity Induced Convection

A He-rich zone, as the one left by the shell H-burning, has a significantly lower opacity than an H-rich zone, at

Downloaded from https://www.cambridge.org/core. IP address: 54.174.225.82, on 22 Jan 2022 at 10:02:55, subject to the Cambridge Core terms of use, available at https://www.cambridge.org/core/terms.
https://doi.org/10.1071/AS03041

the same temperature and pressure. Thus, when the innermost layer of the convective envelope (H-rich) penetrates into the region of decreasing H and increasing He (at the epoch of the TDU), the local value of the radiative opacity increases. Since the radiative gradient (∇_{rad}) is proportional to the opacity, the condition $\nabla_{rad} \gg \nabla_{ad}$ (where ∇_{ad} is the adiabatic temperature gradient) takes place at the base of the convective envelope. In this case, the internal boundary of the convective zone becomes unstable (Becker & Iben 1979; Castellani, Chieffi, & Straniero 1990; Frost & Lattanzio 1996; Castellani, Marconi, & Straniero 1998). In fact, even a small perturbation may increase ∇_{rad} in the formally stable region, immediately below the convective envelope, which then immediately becomes convectively unstable.

A satisfactory treatment of this phenomenon has not yet been found. However, its overall effect on AGB stellar models may be approximated by applying a small perturbation to the boundaries of the convective regions. As a tentative scheme, we have supposed that the velocity of the convective elements (usually evaluated by means of mixing length theory) does not abruptly drop to 0 at the convective boundary, but decreases following an exponential decline law (for more details on the mixing algorithm see Section 2 of Chieffi et al. 2001):

$$v = v_{bce} \exp\left(-\frac{z}{\beta H_P}\right) \quad (8)$$

where v_{bce} is the average velocity at the convective boundary, z is the distance from the convective boundary, H_P the pressure scale-height at the convective boundary and β is a free parameter that controls the steepness of the velocity decline. Usually, when the convective boundary is located within a chemically homogeneous region, $v_{bce} \sim 0$ and the convective border is stable. However, during the TDU, at the base of the convective envelope, the difference between ∇_{rad} and ∇_{ad} increases. Thus, v_{bce} increases, causing an inward propagation of the convective instability. The final result is a substantial increase in the efficiency of the TDU. With $\beta = 0.1$, for example, the amount of H-depleted mass dredged up by convection is about a factor of two larger than that found in models without the exponential decline of the convective velocity (Cristallo et al. 2003).

Some additional models have been computed by setting $\beta = 0.1$ (see Table 1, column 5). The effect on the minimum mass for C-star progenitors is shown in Fig. 2, for the case of solar-composition models. The corresponding decrease of the minimum C-star luminosity is illustrated in Fig. 4.

4 Final Remarks

Based on an homogeneous grid of low-mass AGB stellar models, we have provided interpolation formulae for the basic ingredients of nucleosynthesis calculations. These formulae are strictly valid for $M \leq 3\,M_{\odot}$, at solar metallicity, and for $M \leq 2.5\,M_{\odot}$, in the metallicity range $0.003 \leq Z < 0.02$.

A study of the TDU as a function of total mass and metallicity has been recently published by Karakas, Lattanzio, & Pols (2002), while a comparison of the AGB stellar models computed by means of different evolutionary codes has been discussed by Lugaro et al. (2003). Once the same mass-loss rate is adopted, a substantial agreement is found between our (FRANEC) results and those obtained by using the Mount Stromlo Stellar Structure Program (Frost & Lattanzio 1996; Karakas et al. 2002).

As a final remark, note that, although we have used a Reimers formula to evaluate the mass loss, the fitting formulae are given as a function of the envelope and core masses, and they can be used for any mass-loss law.

Acknowledgments

This research was supported by the Italian grant MURST-FIRB, by the Spanish grant AYA2002-04094-C3-03 and by the Andalusian grant FQM-292.

References

Abia, C., Busso, M., Gallino, R., Domínguez, I., Straniero, O., & Isern, J. 2001, ApJ, 559, 1117
Abia, C., Domínguez, I., Busso, M., Gallino, R., Masera, S., Straniero, O., de Laverny, P., Plez, B., & Isern, J. 2002, ApJ, 579, 817
Becker, S. A., & Iben, I. Jr. 1979, ApJ, 232, 831
Busso, M., Gallino, R., Lambert, D. L., Travaglio, C., & Smith, V. V. 2001, ApJ, 557, 802
Busso, M., Gallino, R., & Wasserburg, G. J. 1999, ARAA, 37, 239
Castellani, V., Chieffi, A., & Straniero, O. 1990, ApJS, 74, 463
Castellani, V., Marconi, M., & Straniero, O. 1998, A&A, 340, 160
Chieffi, A., Dominguez, I., Limongi, M., & Straniero, O. 2001, ApJ, 554, 1159
Cristallo, S., Gallino, R., & Straniero, O. 2003, Mem. SAIt (in press)
Frost, C., & Lattanzio, J. C. 1996, ApJ, 473, 383
Fusi Pecci, F., & Renzini, A. 1976, A&A, 46, 447
Gallino, R., Arlandini, C., Busso, M., Lugaro, M., Travagio, C., Straniero, O., Chieffi, A., & Limongi, M. 1998, ApJ, 497, 388
Gallino, R., Busso, M., & Lugaro, M. 1997, in *Astrophysical Implications of the Laboratory Study of Presolar Material*, eds T. J. Bernatowicz & E. Zinner, *AIP Conf. Proc.*, 402 (Woodbury: American Institute of Physics), 115
Karakas, A. I., Lattanzio, J. C., & Pols, O. R. 2002, PASA, 19, 515
Lambert, D. L., Smith, V. V., Busso, M., Gallino, R., & Straniero, O. 1995, ApJ, 450, 302
Lugaro, M., Herwig, F., Lattanzio, J. C., Gallino, R., & Straniero, O. 2003, ApJ, 586, 1305
Reimers, D. 1975, in *Problems in Stellar Atmospheres and Envelopes*, eds B. Baschek, W. H. Kegel, & G. Traving (Berlin: Springer), 229
Straniero, O., Gallino, R., Busso, M., Chieffi, A., Limongi, M., & Salaris, M. 1995, ApJ, 440, L85
Straniero, O., Chieffi, A., Limongi, M., Gallino, R., Busso, M., & Arlandini, C. 1997, ApJ, 478, 332

Downloaded from https://www.cambridge.org/core. IP address: 54.174.225.82, on 22 Jan 2022 at 10:02:55, subject to the Cambridge Core terms of use, available at https://www.cambridge.org/core/terms. https://doi.org/10.1071/AS03041